Striking isotope effect on the metallization phase lines of liquid hydrogen and deuterium

Mohamed Zaghoo,[*] Rachel J. Husband,[†] and Isaac F. Silvera[‡]
Lyman Laboratory of Physics, Harvard University, Cambridge, Massachusetts 02138, USA

(Received 12 May 2018; revised manuscript received 9 August 2018; published 4 September 2018)

Liquid atomic metallic hydrogen is the simplest, lightest, and most abundant of all liquid metals. The importance of nucleon motions or ion dynamics can be studied by comparing the metallization phase lines of the dissociative insulator-metal transitions of hydrogen and deuterium. We use static compression to study the optical properties of dense liquid metallic deuterium in the pressure region of 1.2–1.7 Mbars and measured temperatures up to ∼3000 K. At the same pressure (density) for the two isotopes, the phase lines of this transition reveal a prominent isotopic shift of ∼700 K. Our paper shows the importance of quantum nuclear effects in the metallization transition and conduction properties in dense hydrogen isotopes at conditions of giant planetary interiors and provides an invaluable benchmark for *ab initio* calculations.

DOI: 10.1103/PhysRevB.98.104102

I. INTRODUCTION

As the lightest atoms, hydrogen and its isotopes exhibit the largest mass ratios of the elements, giving rise to large differences in their properties. The binding energies of the homonuclear free molecules H_2 and D_2 differ by ∼900 K (4.477eV for H_2 and 4.556 eV for D_2) [1]. The isotopic shift in the binding energy is related to the different zero-point energies (ZPEs) arising from the fundamental vibrational mode of the molecules. Due to their ZPEs, at low temperatures (T) where both hydrogen and deuterium form quantum solids, large isotopic effects are manifested in phonon, vibrational, and rotational excitations as well as in their equations of state and melting temperatures [2]. In 1935, Wigner and Huntington first discussed the role of density in destabilizing the molecular bond in the crystalline phase, predicting a dissociative transition to metallic hydrogen (MH) at sufficient compression in the low-temperature limit [3]. This transition has recently been reported in hydrogen at low temperatures by Dias and Silvera [4]. In the high-temperature high-density fluid phase, a liquid-liquid insulator-to-metal transition (LLIMT) has long been studied to describe molecular hydrogen's transition to atomic liquid metallic hydrogen [5,6], also called the plasma phase transition (PPT) [7–14]. The LLIMT locates the boundary between a molecular fluid and an atomic MH in astrophysical gas giants, a central characteristic of all interior model structures of Jovian-like planets [15]. Due to its fundamental nature as well as its astrophysical significance, the precise location and nature of this phase line remains the subject of intense theoretical and experimental research.

There are two experimental techniques that have been used to study the high-temperature metallization of the hydrogen isotopes: (1) dynamic compression that can pressurize and heat the sample for a few to tens of nanoseconds, depending on the technique, and (2) static compression with diamond-anvil cells (DACs) that produce high pressures and high temperatures using cw or pulsed-laser heating that lasts a few hundred nanoseconds. The thermodynamic pathway can either cross the first-order phase line or enter the metallic phase below the critical pressure or above the critical temperature where the transition is continuous. In dynamic compression experiments designed for temperatures of a few thousand degrees K, the temperature is not measured but almost always estimated theoretically, whereas in DACs, T is measured experimentally. Weir *et al.* [16] used reverberating shocks to isentropically compress H_2 and D_2 (to probe lower temperatures) while measuring electrical conductivities, observing a continuous transition to the metallic state. Either their sensitivity was insufficient to detect the phase line (so the transition is at a lower pressure than their end point) or they metallize below the critical point. They point out that gas gun experiments are not designed to probe isotope effects; the initial mass densities differ by 2.4, so their final molar densities and temperatures differ substantially at the same final pressure [17]. Celliers *et al.* [18] used laser-driven shock waves to observe liquid metallic deuterium by its reflectance, and Loubeyre *et al.* [19] used laser-driven shocks of hydrogen and deuterium in diamond-anvil cells to observe metallic reflectance at very high temperatures. In both cases the metallic state was evidently entered below the critical pressure without crossing the phase line. Fortov *et al.* [20] and Mochalov *et al.* [21], using explosive isentropic compression of deuterium, reported density discontinuities attributed to the PPT at approximately the same pressure as Weir *et al.* [16]. All of these data points have large uncertainties in temperatures of order ±500–1000 K since they are calculated. Knudson *et al.* [22] implemented quasi-isentropic magnetically driven ramp compression of deuterium to probe lower temperatures (still thousands of degrees K) and reported a phase line based on an abrupt rise in reflectance, which is at much higher pressures than previous dynamic studies of deuterium. Both pressure and temperature were calculated from equation of state models (with no experimental uncertainties), and the sample was observed to first become absorptive and then reflective during

[*]Current address: Laboratory for Laser Energetics, University of Rochester, New York 14620, USA.
[†]Current address: Photon Sciences, Deutsches Elektron Synchrotron, Hamburg, Germany.
[‡]silvera@physics.harvard.edu

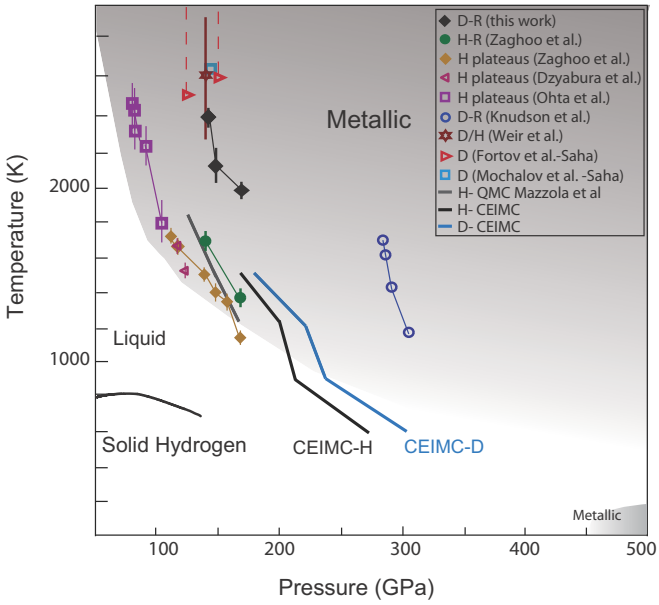

FIG. 1. The high-T hydrogen deuterium phase diagram showing experimental data and theoretical predictions of the insulator-metal phase boundary in the fluid phase, all identified in the legend. Our deuterium data points (solid black diamonds) delineating a phase boundary are based on the optical signature of an abrupt rise in reflectance. Systematic uncertainties in the temperature are discussed elsewhere (see the Supplemental Material [29]). The filled circles indicate the onset of reflectance from our previous hydrogen studies; the smaller filled diamonds show the phase line based on observation of plateaus [24,25]. The P-T values where static experiments reported metallization in the low-temperature limit are also shown in the lower right corner [4]. The solid lines indicate theoretical CEIMC predictions for the PPT phase lines in hydrogen and deuterium [12]. The open circles are due to Knudson *et al*.

the compression. As can be seen in Fig. 1, there seems to be a large inconsistency between the shock measurements.

The location of the phase line of hydrogen was determined in DACs by Dzyabura *et al.* [23] and Ohta *et al.* [24], based on observed plateaus in heating curves (plots of peak temperature vs laser power). In order to show that these plateaus were a signature of the transition to metallic hydrogen, Zaghoo *et al.* [25] and Zaghoo and Silvera [26] studied the optical properties of pulsed-laser-heated hydrogen, reporting abrupt changes in these properties at the phase line, consistent with metallization. The transition was identified by absorption of light that coincided with the onset of the plateaus, whereas the rise in reflectance was observed above the plateau temperature (Fig. 1).

Early theoretical studies differed in their predictions of the LLIMT boundary by as much as 4 Mbars in pressure (P) and ∼10 000 K in T. All theories predict the transition to be first order with latent heat, a negative P-T slope, and a critical point at the low-P, high-T side of the line. Studies were focused on hydrogen and did not explicitly consider the heavier isotopes. Although many theoretical studies treat the protons classically in the warm dense fluid [8,10], the inclusion of nuclear quantum effects can significantly alter the location of the phase line (see the discussion in Ref. [27]). Recently the phase lines for isotopes were calculated using coupled electron-ion Monte Carlo (CEIMC) [12] which treats the ions quantum mechanically (Fig. 1). Results for hydrogen were in excellent agreement with the phase line determined by static compression techniques [25] but indicated a small isothermal shift for deuterium on the order of ∼ 20–40 GPa or an isobaric shift of ∼100–200 K.

II. EXPERIMENTAL

In Fig. 1 we see that there is a clear spread of experimental results. The pressure of the phase line of deuterium observed by Knudson *et al.* [22] differs substantially from other dynamic measurements and is ∼125 GPa higher than the line observed in static compression experiments on hydrogen. In order to resolve these differences we have measured the transition line to the liquid metallic state of deuterium using the same experimental method that was previously used for hydrogen [25,26]. This enables us to make a comparison of the two isotopes, while eliminating possible systematic uncertainties that may exist when comparing data collected using different techniques or different criteria for the onset of the transition. Valid comparisons of the two isotopes must be made at the same molar density. We note that at a given pressure (at high pressures) the difference in isotopic molar densities is negligible [28]. If an isotope effect exists due to nuclear quantum effects then this should be observable by comparing the phase lines of the two isotopes. Thus, comparing our phase lines for H_2 and D_2 in Fig. 1 at a given pressure we observe a shift of phase lines on the order of 700 K in the metallization temperatures. We attribute this shift to the different dissociation energies in the high-density liquids that arise from different zero-point energies. Clearly, there is a large disagreement with the line of Knudson *et al.* [22].

In order to observe the phase line, we have performed optical studies of statically compressed deuterium samples in the pressure range of 124–169 GPa and temperatures up to ∼3000 K using pulsed laser heating. A schematic of the DAC interior is shown in Fig. 2. The diamond/gasket assembly was coated with an ∼50-nm amorphous alumina layer serving as a hydrogen diffusion barrier. A thin semitransparent tungsten (W) film (∼8.5–11-nm thick) was deposited onto the lower diamond to act as an absorber for laser heating; this was coated with an ∼5-nm amorphous alumina protective layer to inhibit diffusion into the W film. Samples were indirectly heated using a Nd:YAG laser (1064 nm) with a 20-kHz repetition rate and a ∼280-ns pulse width. This is long enough to achieve local thermal equilibrium in the heated deuterium but sufficiently short to further suppress hydrogen diffusion. Temperature was determined by fitting the emitted thermal irradiance spectra to Planckian curves (see the Supplemental Material [29]). Examples of the raw data and the fitted region are shown in Fig. 2. An advantage of the work reported here over our earlier studies on hydrogen is that the deuterium fundamental vibron Q_1 mode falls within the spectral range of our InGaAs diode array detector (Fig. 2). This enabled us to monitor the vibron and thus the integrity of our deuterium samples as a function of increasing temperature. Pressure was determined from the Raman shift of the deuterium vibron at room temperature with an uncertainty of ±2 GPa using a calibration from Mao and Hemley [30].

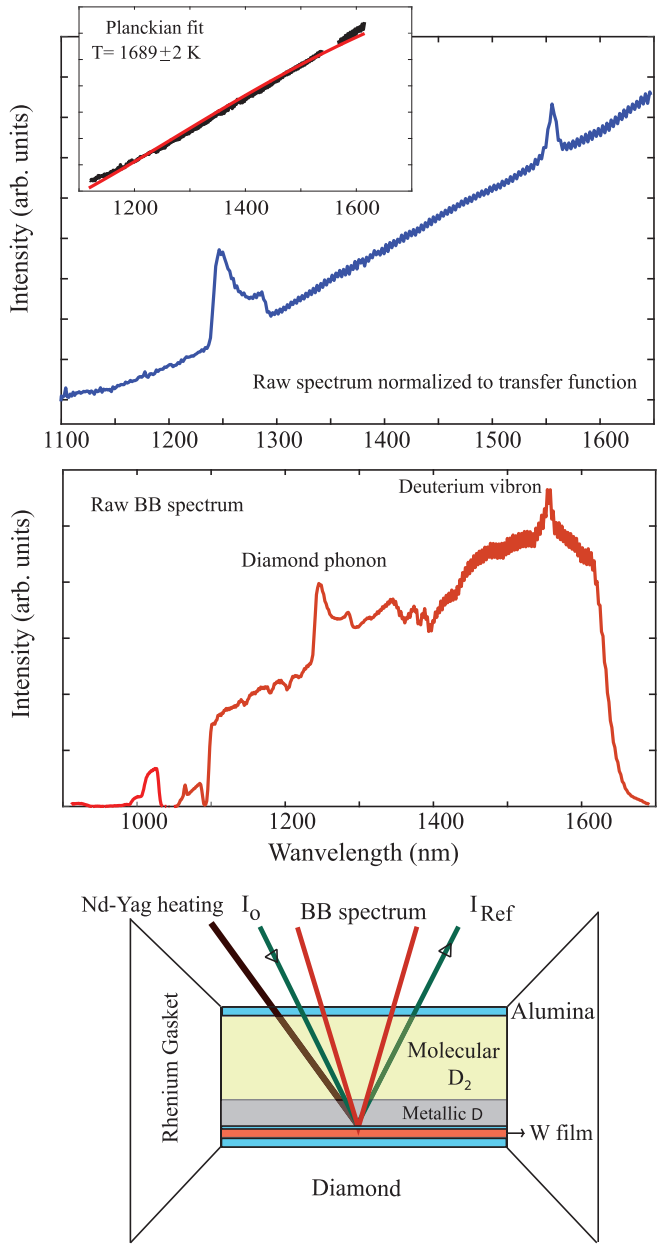

FIG. 2. Bottom: schematic of the DAC interior showing the arrangement for pyrometry and reflectance measurements (not to scale). Middle: typical spectral irradiance spectrum recorded on our infrared InGaAs diode array detector, showing the diamond phonon, deuterium vibron, as well as the rising slope of the blackbody radiation. Top: the same spectrum shown in the middle panel normalized by the transfer function to correct for the optical response of our setup. After subtracting the diamond and vibron features using a procedure described elsewhere [23], the data are fit to a Planck curve to determine the temperature. The pressure was 142 GPa. Larger possible systematic uncertainties are discussed in the Supplemental Material Ref. [29]).

The peak temperature of the deuterium sample was gradually increased by incrementally increasing the laser power or energy/pulse of our heating laser to probe the phase line. Time-resolved reflectance of light from one or two cw probe lasers (514.5 and 980 nm) was measured using Si photodetectors with a 3-ns rise time. Unlike dynamic studies of the PPT, the photon energy dependence of optical reflectance was measured simultaneously with measurements of the temperature. Example reflectance traces, collected with increasing temperature at 142 GPa, are shown in Fig. 3. For times before the heating laser pulse, the trace shows the reflectance signal from the tungsten absorber R_W. At temperatures below the transition, deuterium remains transparent, and no detectable change is observed in the reflectance trace. Above the transition temperature, a sharp rise in reflectance is observed due to the formation of liquid metallic deuterium (LMD), consistent with a first-order phase transition (see the Supplemental Material [29]). At the threshold of the transition, the LMD film is thin enough so that it is partially transparent. As the laser power is increased, the film thickens, and the reflectance signal rapidly increases.

In order to better compare with the majority of dynamic studies that use reflectance as the signature of metallization, in this paper we use the onset of reflectance as the criterion for the phase line. Figure 1 shows our P-T points for the onset of the highly reflecting/conducting state in liquid deuterium and can be compared to results for hydrogen. The deuterium reflectance was determined in accordance with the method used for hydrogen [25]. The relationship between the normalized reflectance signal R_S and the LMD reflectance R is given by $R_S = R/R_W + Tr^2$. Here, R_W is the reflectance of the tungsten, and Tr is the transmission of the LMD film. For thick films, Tr approaches zero, and $R = R_W R_S$. Our reflectance data are summarized in Fig. 4 and compared to hydrogen. The highest values of our measured reflectances for LMD are around 0.5–0.6, overlapping the values found for reflectance in dynamic experiments [18,19,22] and bulk hydrogen films [26]. We note that the onset of the reflectance of deuterium is much sharper than hydrogen (see the discussion in the Supplemental Material [29]).

III. DRUDE FREE-ELECTRON ANALYSIS

Optical reflectance data are amenable to the Drude free-electron analysis which has two parameters: the plasma frequency ω_p, where $\omega_p^2 = 4\pi e^2 n_e/m_e$, and the scattering time τ. Here n_e and m_e are the electron density and mass. The measured reflectance for a thick metallic film at a given frequency is $R(\omega) = |(N_{\rm diam} - N_D)/(N_{\rm diam} + N_D)|^2$, where $N_{\rm diam}$ is the index of refraction of the molecular deuterium/diamond layer and N_D is the complex index of refraction of LMD: $N_D^2 = 1 - \omega_p^2/(\omega^2 + j\omega/\tau)$. We performed a least-squares nonlinear fit of our measured $R(\omega)$ to extract the plasma frequency ω_p and the scattering time τ (Fig. 4, lower right panel). As the pressure or temperature increases beyond the onset region, LMD becomes Drude-like, and when the carriers are degenerate, the free-electron character is established. At 142 GPa and 2442 K, the data are best fit to $\omega_p = 21.3 \pm 0.9$ eV and τ of $1.7 \pm 0.2 \times 10^{-16}$ s; the dissociation fraction is 0.70 ± 0.06, calculated from the plasma frequency and the atomic density [28]. We contrast our measured reflectance to that expected in the Mott-Ioffe-Regel minimum metallic conductivity limit (with full dissociation). This defines the minimum value of conductivity and corresponds to a mean free path equal to the average interatomic distance a. The expected reflectance in this limit is plotted alongside our data in Fig. 4 and clearly

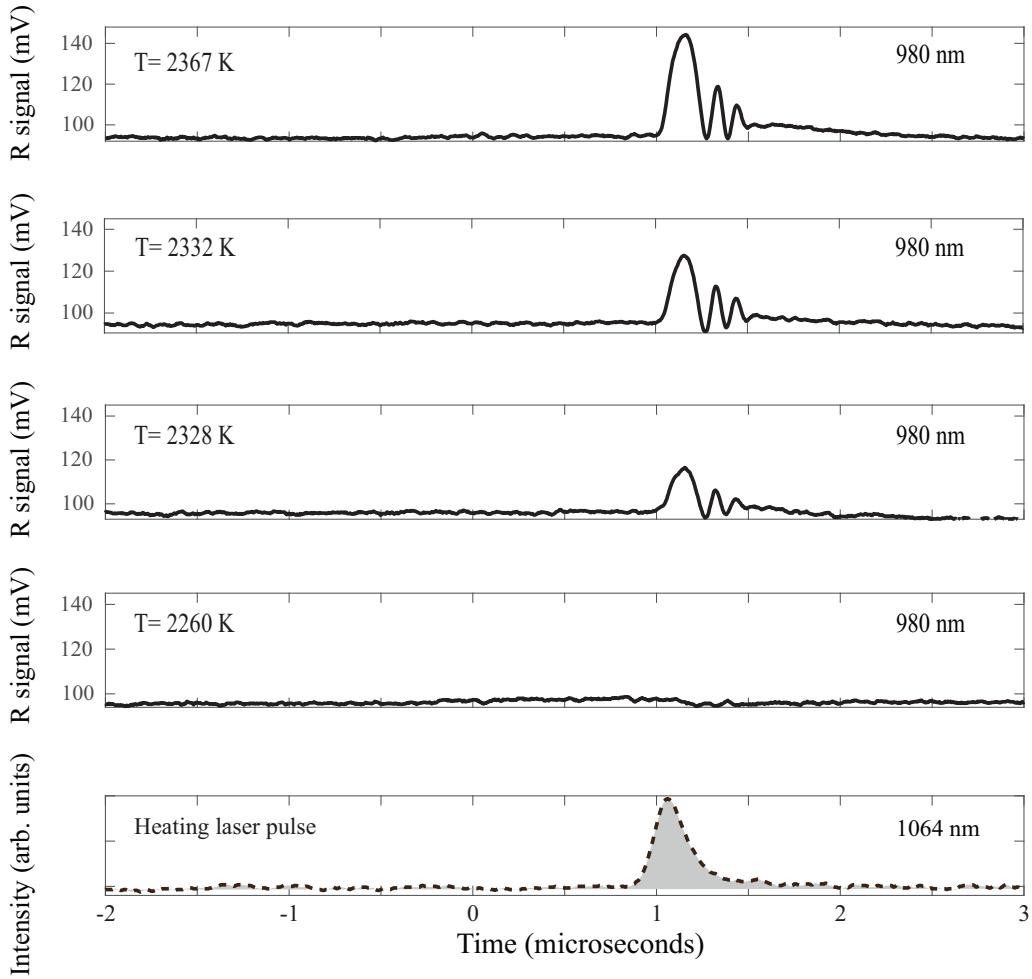

FIG. 3. Example of the raw time-resolved reflectance traces recorded as a function of temperature and time for 980-nm light and $P = 142$ GPa. The bottom panel shows the timing of the heating laser-pulse 1064 nm. Above a certain temperature, liquid deuterium abruptly metallizes and reflects the incident probe light. Increased heating thickens the metallic layer that reflects more light. The secondary peaks are due to optical interference in the metallic deuterium/diamond interfaces.

cannot account for the high values of reflectance observed in this paper.

IV. PHASE TRANSITION LINE AND ISOTOPIC SHIFTS

Our transition points are plotted in Fig. 1 and can be compared to results for hydrogen. Although our current data do not extend to high enough pressures to make a comparison isothermally, at the same pressure, we find an isotopic shift on the order of ∼700 K. The magnitude of the shift is consistent with the difference in the ZPEs of the vibrational energies of the two species at high density (see the statistical estimate in the Supplemental Material [29]). This is striking, considering the complex many-body effects, strong coupling, and thermal degeneracy present in the dense fluid state. A negative slope of the metallization phase line revealed from our data is supportive of the dissociation model; the dissociation energy decreases with density, and thus the transition temperature decreases. We note that at high pressure the molar volumes of the two isotopes are the same at a given pressure [28]. Thus a mechanism of metallization by electronic band overlap [31] at a transition density cannot account for the observed isotopic shift. Equal molar volumes would imply identical transition pressures since the isotopes are isoelectronic. Our hydrogen metallization phase line (based on the onset of reflectance) is in rather good agreement with the most recent theoretical results [12,14], however the CEIMC calculation [12] appears to underestimate the observed isotope shift.

In addition to revealing a fundamental effect in the metallization phase line in the dense hydrogen isotopes, our results with measured temperatures could help to resolve the conflicting results in dynamic experiments. As shown in Fig. 1, our deuterium phase line is in good agreement with earlier shockwave studies on deuterium [16,20,21], albeit their large temperature uncertainties. Our data are also consistent with the new laser compression experiments at the National Ignition Facility that identified metallization in compressed deuterium at 200 GPa and above 1000 K [32]. There is a large apparent discrepancy with the phase line of Knudson *et al.* [22]. We suspect that their temperature estimation is at fault. If their calculated temperatures were scaled to lower values, their data might fall onto an extrapolation of our

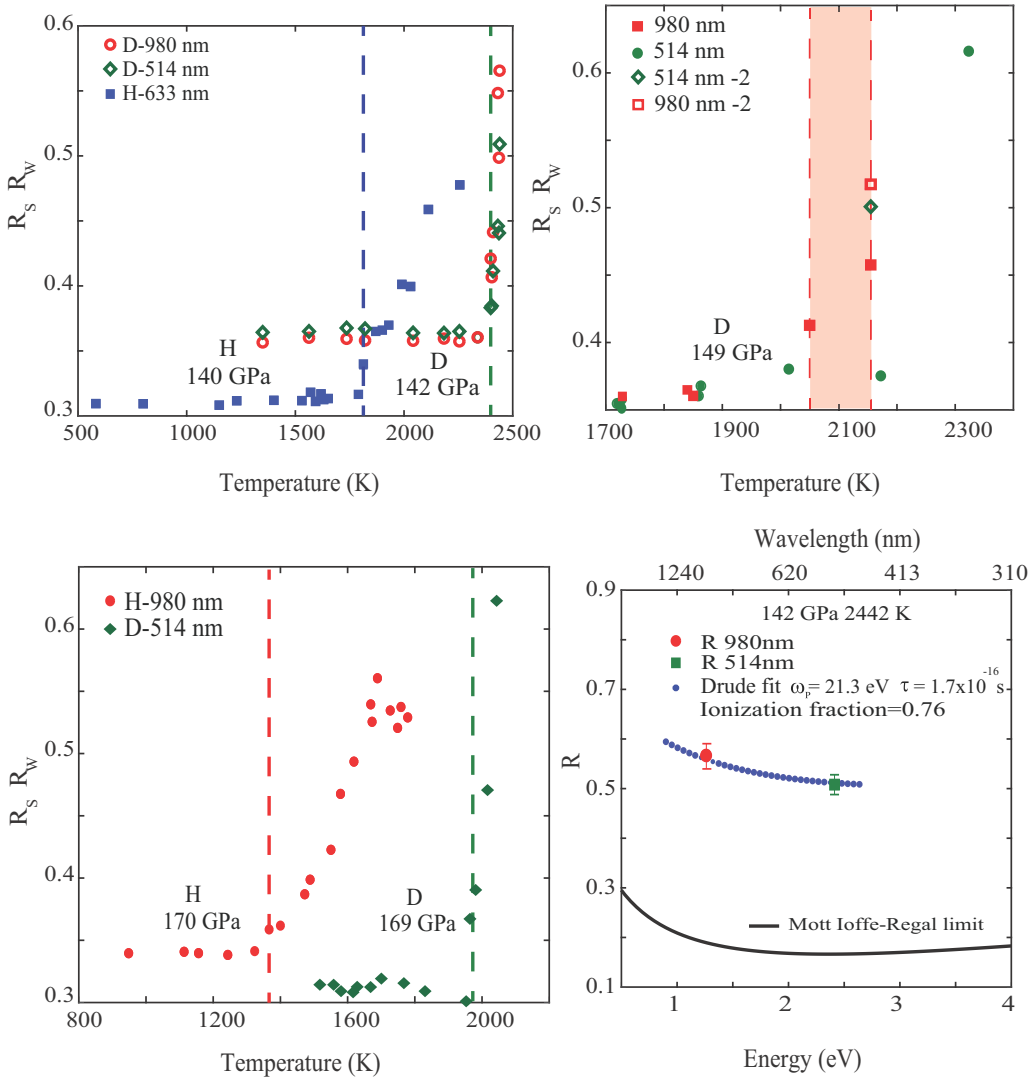

FIG. 4. Top and bottom left: reflectance signal of deuterium and hydrogen [26] on a W film vs T for various pressures. Both isotopes reflect more light at increasing wavelengths, consistent with the free-electron model. The open symbols represent data in which reflectance was measured simultaneously at two wavelengths. For the 149-GPa data the open symbols denote a different run than the filled ones. We plot the reflectance signal times the reflectance of the tungsten film. This is equal to the metallic reflectance of the isotope for thick films (see the Supplemental Material [29]). The abscissas are a measure of the reflectance of W below the transition and the reflectance of liquid metals for thick films. For the deuterium we estimate a possible systematic uncertainty of 10% for the reflectance of the tungsten film; this is larger than the random errors so we do not show error bars. Random temperature uncertainties are small (see the Supplemental Material [29]). Bottom right: the Drude fit to the experimental data derived from a least-squares fit to the energy dependence of measured reflectance. The solid line is the calculated reflectance using the Mott-Ioffe-Regal limit, assuming full dissociation. The vertical lines indicate the T values for the transition, based on the onset of reflectance.

deuterium phase line. Modeling of interior planetary structures of Jovian-like planets where hydrogen (not deuterium) is the primary constituent should thus rely on the previous static pressure [25,26] determination of the PPT phase line.

V. DISCUSSION

The most recent magnetic measurements from the Juno space mission are also supportive of this conclusion where the Jovian dynamo action is revealed to operate at much shallower depths than previously estimated [33,34], consistent with our hydrogen metallization line reported at lower pressures [26]. Furthermore, our paper suggests the importance of nuclear quantum effects in describing the electronic and thermodynamic states of planetary interior hydrogen-rich dense warm ices, such as water, methane, or ammonia. If so, then current thermal and magnetic models of ice giants [35], which have thus far relied on *ab initio* density functional theory methods implementing classical ions, may require revision.

ACKNOWLEDGMENTS

The NSF, Grant No. DMR-1308641, the DOE Stockpile Stewardship Academic Alliance Program, Grant No.

DE-NA0003346, and the NASA Earth and Space Science Fellowship Program, Award No. NNX14AP17H supported this research. The preparation of the diamond surfaces was performed, in part, at the Center for Nanoscale Systems (CNS), a member of the National Nanotechnology Infrastructure Network, which is supported by the National Science Foundation under NSF Award No. ECS-0335765. CNS is part of Harvard University.

[1] G. Herzberg and A. Monfils, The dissociation energies of the H2, HD, and D2 molecules, J. Mol. Spectrosc. **5**, 482 (1960).

[2] I. F. Silvera, The solid molecular hydrogens in the condensed phase: Fundamentals and static properties, Rev. Mod. Phys. **52**, 393 (1980).

[3] E. Wigner and H. B. Huntington, On the possibility of a metallic modification of hydrogen, J. Chem. Phys. **3**, 764 (1935).

[4] R. Dias and I. F. Silvera, Observation of the Wigner-Huntington transition to solid metallic hydrogen, Science **355**, 715 (2017).

[5] G. E. Norman and A. N. Starostin, The invalidity of the classsical description of a non-degnerated dense plasma, Teplofiz. Vys. Temp. **6**, 410 (1968).

[6] W. Ebeling and W. Richert, Plasma phase transition in hydrogen, Phys. Lett. A **108**, 80 (1985).

[7] D. Saumon and G. Chabrier, Fluid Hydrogen at High Density: The Plasma Phase Transition, Phys. Rev. Lett. **62**, 2397 (1989).

[8] S. Scandolo, Liquid-liquid phase transitions in compressed hydrogen from first-principles simulations, Proc. Natl. Acad. Sci. USA **100**, 3051 (2003).

[9] M. A. Morales, C. Pierleoni, E. Schwegler, and D. M. Ceperley, Evidence for a first order liquid-liquid transition in high pressure hydrogen from ab-initio simulations, Proc. Natl. Acad. Sci. USA **107**, 12799 (2010).

[10] W. Lorenzen, B. Holst, and R. Redmer, First-order liquid-liquid phase transition in dense hydrogen, Phys. Rev. B **82**, 195107 (2010).

[11] M. A. Morales, J. M. McMahon, C. Pierleoni, and D. M. Ceperley, Nuclear Quantum Effects and Nonlocal Exchange-Correlation Functionals Applied to Liquid Hydrogen at High Pressure, Phys. Rev. Lett. **110**, 065702 (2013).

[12] C. Pierleoni, M. A. Morales, G. Rillo, M. A. Strzhemechny, M. Holzmann, and D. M. Ceperley, Liquid–liquid phase transition in hydrogen by coupled electron–ion Monte Carlo simulations, Proc. Natl. Acad. Sci. USA **113**, 4953 (2016).

[13] R. S. McWilliams, D. A. Dalton, M. F. Mahmood, and A. F. Goncharov, Optical Properties of Fluid Hydrogen at the Transition to a Conducting State, Phys. Rev. Lett. **116**, 255501 (2016).

[14] G. Mazzola, R. Helled, and S. Sorella, Phase Diagram of Hydrogen and a Hydrogen-Helium Mixture at Planetary Conditions by Quantum Monte Carlo Simulations, Phys. Rev. Lett. **120**, 025701 (2018).

[15] T. Guillot, The interiors of giant Planets: Models & outstanding questions, Annu. Rev. Earth Planet. Sci. **33**, 493 (2005).

[16] S. T. Weir, A. C. Mitchell, and W. J. Nellis, Metallization of Fluid Molecular Hydrogen at 140 GPa (1.4 Mbar), Phys. Rev. Lett. **76**, 1860 (1996).

[17] W. J. Nellis, S. T. Weir, and A. C. Mitchell, Minimum metallic conductivity of fluid hydrogen at 140 GPa (1.4 Mbar), Phys. Rev. B **59**, 3434 (1999).

[18] P. M. Celliers, G. W. Collins, L. B. D. Silva, D. M. Gold, R. Cauble, R. J. Wallace, M. E. Foord, and B. A. Hammel, Shock-Induced Transformation of Liquid Deuterium into a Metallic Fluid, Phys. Rev. Lett. **84**, 5564 (2000).

[19] P. Loubeyre, S. Brygoo, J. Eggert, P. M. Celliers, D. K. Spaulding, J. R. Rygg, T. R. Boehly, G. W. Collins, and R. Jeanloz, Extended data set for the equation of state of warm dense hydrogen isotopes, Phys. Rev. B **86**, 144115 (2012).

[20] V. E. Fortov R. I. Ilkaev, V. A. Arinin, V. V. Burtzev, V. A. Golubev, I. L. Iosilevskiy, V. V. Khrustalev, A. L. Mikhailov, M. A. Mochalov, V. Ya. Ternovoi, and M. V. Zhernokletov, Phase Transition in a Strongly Nonideal Deuterium Plasma Generated by Quasi-Isentropical Compression at Megabar Pressures, Phys. Rev. Lett. **99**, 185001 (2007).

[21] M. A. Mochalov, R. I. Il'kaev, V. E. Fortov, A. L. Mikhailov, A. O. Blikov, V. A. Ogorodnikov, V. K. Gryaznov, and I. L. Iosilevskii, Quasi-isentropic compressibility of a strongly nonideal deuterium plasma at pressures of up to 5500 Gpa: Nonideality and degeneracy effects, J. Exp. Theor. Phys. **124**, 505 (2017).

[22] M. D. Knudson, M. P. Desjarlais, A. Becker, R. W. Lemke, K. R. Cochrane, M. E. Savage, D. E. Bliss, T. R. Mattsson, and R. Redmer, Direct observation of an abrupt insulator-to-metal transition in dense liquid deuterium, Science **348**, 1455 (2015).

[23] V. Dzyabura, M. Zaghoo, and I. F. Silvera, Evidence of a liquid-liquid phase transition in hot dense hydrogen, Proc. Natl. Acad. Sci. USA **110**, 8040 (2013).

[24] K. Ohta, K. Ichimaru, M. Einaga, S. Kawaguchi, K. Shimizu, T. Matsuoka, N. Hirao, and Y. Ohishi, Phase boundary of hot dense fluid hydrogen, Sci. Rep. **5**, 16560 (2015).

[25] M. M. Zaghoo, A. Salamat, and I. F. Silvera, Evidence of a first-order phase transition to metallic hydrogen, Phys. Rev. B **93**, 155128 (2016).

[26] M. Zaghoo and I. F. Silvera, Conductivity and dissociation in metallic hydrogen with implications for planetary interiors, Proc. Natl. Acad. Sci. USA **114**, 11873 (2017).

[27] J. M. McMahon, M. A. Morales, C. Pierleoni, and D. M. Ceperley, The properties of hydrogen and helium under extreme conditions, Rev. Mod. Phys. **84**, 1607 (2012).

[28] P. Loubeyre, R. LeToullec, D. Hausermann, M. Hanfland, R. J. Hemley, H. K. Mao, and L. W. Finger, X-ray Diffraction and equation of state of hydrogen at megabar pressures, Nature (London) **383**, 702 (1996).

[29] See Supplemental Material at http://link.aps.org/supplemental/10.1103/PhysRevB.98.104102 for pressure and temperature determination, optical and Drude analysis, isotopic shift analysis, and experimental comparisons, which includes Refs. [36–50].

[30] H. Mao and R. J. Hemley, Ultrahigh-pressure transitions in solid hydrogen, Rev. Mod. Phys. **66**, 671 (1994).

[31] W. J. Nellis, A. A. Louis, and N. W. Ashcroft, Metallization of fluid hydrogen, Philos. Trans. R. Soc. London, Ser. A **356**, 119 (1998).

[32] P. M. Celliers *et al.*, 20th Biennial Conference of the APS Topical Group on Shock Compression of Condensed Matter, St. Louis, 2017 (APS, Ridge, NY, 2017).

[33] S. J. Bolton, A. Adriani, V. Adumitroaie, M. Allison, J. Anderson, S. Atreya, and J. Bloxham, Jupiter's interior and deep atmosphere: The initial pole-to-pole passes with the Juno spacecraft, Science **356**, 821 (2017).

[34] M. Zaghoo and G. W. Collins, Size and strength of self-excited dynamos in Jupiter-like extrasolar planets, ApJ **862**, 19 (2018).

[35] B. Holst, M. French, and R. Redmer, Electronic transport coefficients from ab initio simulations and application to dense liquid hydrogen, Phys. Rev. B **83**, 235120 (2011).

[36] I. F. Silvera and R. J. Wijngaarden, Diamond Anvil cell and cryostat for low temperature optical studies, Rev. Sci. Instrum. **56**, 121 (1985).

[37] S. Rekhi, J. Tempere, and I. F. Silvera, Temperature determination for nanosecond pulsed laser heating, Rev. Sci. Instrum. **74**, 3820 (2003).

[38] S. Deemyad, A. N. Papathanassiou, and I. F. Silvera, Strategy and enhanced temperature determination in a laser heated diamond anvil cell, J. Appl. Phys **105**, 093543 (2009).

[39] S. Deemyad, E. Sterer, C. Barthel, S. Rekhi, J. Tempere, and I. F. Silvera, Pulsed laser heating and temperature determination in a diamond Anvil cell, Rev. Sci. Instrum. **76**, 125104 (2005).

[40] L. Benedetii and P. Loubeyre, Temperature gradients, wavelength-dependent emissivity, and accuracy of high and very-high temperatures measured in the laser-heated diamond cell, High Pressure Res. **24**, 423 (2007).

[41] N. Van den Broeck, F. Brosens, J. Tempere, and I. F. Silvera, Optical properties of inhomogeneous metallic hydrogen plasmas, Phys. Rev. B **93**, 155129 (2016).

[42] W. Evans and I. F. Silvera, Index of refraction, polarizability, and equation of state of solid molecular hydrogen, Phys. Rev. B **57**, 14105 (1998).

[43] O. Pfaffenzeller and D. Hohl, Structure and electrical conductivity in fluid high-density hydrogen, J. Phys.: Condens. Matter **9**, 11023 (1997).

[44] F. Lin, M. A. Morales, K. T. Delaney, C. Pierleoni, R. M. Martin, and D. M. Ceperley, Electrical Conductivity of High-Pressure Liquid Hydrogen By Quantum Monte Carlo Methods, Phys. Rev. Lett. **103**, 256401 (2009).

[45] K. K. Irikura, Experimental vibrational zero-point energies: diatomic molecules, J. Phys. Chem. Ref. Data **36**, 389 (2007).

[46] A. F. Goncharov and J. C. Crowhurst, Raman Spectroscopy of Hot Compressed Hydrogen and Nitrogen: Implications for the Intramolecular Potential, Phys. Rev. Lett. **96**, 055504 (2006).

[47] N. Subramanian, A. V. Goncharov, V. V. Struzhkin, M. Somayazulu, and R. J. Hemley, Bonding changes in hot fluid hydrogen at megabar pressures, Proc. Natl. Acad. Sci. USA **108**, 6014 (2011).

[48] L. Caillabet, S. Mazevet, and P. Loubeyre, Multiphase equation of state of hydrogen from ab initio calculations in the range 0.2 to 5 g/cc up to 10 eV, Phys. Rev. B **83**, 094101 (2011).

[49] S. Brygoo, M. Millot, P. Loubeyre, P. Celliers, G. Collins, J. Eggert, R. Rygg, D. Swift, and R. Jeanloz, 20th Biennial Conference of the APS Topical Group on Shock Compression of Condensed Matter, St. Louis, 2017 (APS, Ridge, NY, 2017).

[50] I. F. Silvera, R. Husband, A. Salamat, and M. Zaghoo, Expanded Comment on: Optical Properties of Fluid Hydrogen at the Transition to a Conducting State, Condensed matter, arXiv:1608.04479.